

Towards Commodity, Web-Based Augmented Reality Applications for Research and Education in Chemistry and Structural Biology

Luciano A. Abriata*

École Polytechnique Fédérale de Lausanne, Lausanne, Switzerland

luciano.abriata@epfl.ch

ABSTRACT

This article reports proof-of-concept web apps that use commodity open-source technologies for augmented and virtual reality to tackle real-world problems from chemistry and structural biology. The apps include demonstrations of molecular visualization at atomistic and coarse-grained levels, coarse-grained modeling of molecular physics, on-the-fly calculation of experimental observables and comparison to actual data, and simulated chemical reactivity. Along the results and in the discussion section, future perspectives are depicted based on recent works in the areas of machine learning for chemistry, transcompilation of programs into JavaScript, and advanced APIs and libraries supported by major web browsers. Together, the developments presented and discussed in this article will certainly lead to the next generation of tools for truly interactive molecular modeling that can streamline human thought and intent with the numerical processing power of computers.

Keywords: Augmented reality, mixed reality, molecular visualization, molecular graphics, human-computer interaction, molecular modeling, molecular simulations, chemistry, biology, structural biology, biophysics, coarse-grained, molecular dynamics.

1 INTRODUCTION

Immersive virtual reality (VR) and in particular augmented reality (AR) have enormous potential for assisting scientific research and education, especially in disciplines that deal with abstract objects, objects much smaller or larger than human dimensions, or objects that are hard to acquire and handle due to high costs, limited availability, fragility, etc.[1]–[4] Chemistry is one such discipline where AR and VR have been attributed high educational and exploratory potentials [1], [2], [5]–[7], although actual reach, user acceptance and educational effects have not

been deeply assessed.[8], [9] Arguably, some of these limitations arise from the complex software setups involved in most current applications, which combine different modules to take camera feeds, analyze markers, calculate molecular data and render overlaid graphics. As I intend to demonstrate here, this and other problems are alleviated when client side web technologies are utilized as the core platform, easily allowing for device-independent, open, inexpensive AR and VR applications in chemistry and related disciplines.

In this article I demonstrate that client side web-based technologies have matured enough to support complete scientific applications based on AR and VR through commodity software and hardware, which educators and researchers can already put into use today, exemplified here with problems from chemistry and the related disciplines of biophysics and structural biology. Somewhat similar applications have been around for some time, but most of them involved complex coupling of multiple programs such as camera feeds, augmented reality marker detection, and molecular graphics rendering [1], [2]. In contrast, being based entirely on open, community-contributed client-side software for building interactive web content, the web apps presented here are on one hand easy to deploy, profiting from several ready-to-use libraries and APIs, and on the other hand freely and fully accessible to users through standard web browsers in multiple devices such as smartphones, tablets and computers, without requiring any installation.[10], [11] Moreover, previous works have focused mainly on visualization largely overlooking molecular dynamics, reactivity and information overlay, except for some notable works like [12], [13]; but as the following proof-of-concept examples show, current technologies allow for in-browser calculations of molecular mechanics, calculations of experimental observables and real-time comparison to actual experimental data, plus

enhanced human-computer interaction including spoken commands, and even more exciting possibilities as discussed by the end of the article.

2 THEORY

The core of these proof-of-concept applications is built around in-browser solutions for AR, VR, and simulation of particle physics, speech recognition and data plotting (Table 1). Virtual reality is achieved through A-Frame, an entity component system framework for Three.js that simplifies creation of 3D and virtual scenes in the web. Marker tracking for virtual reality is achieved through AR.js developed by J. Etienne, which in turn handles rendering of Three.js objects either directly or through A-Frame. Solid body physics are handled through Cannon.js developed by S. Hedman and wrapped into HTML by D. McCurdy. Calculations specific to the problems of interest are coded *ad hoc* in JavaScript. The anyyang speech recognition library by T. Ater is used to process spoken commands, and Google Charts is used for displaying data plots. All relevant URLs pointing to these tools are given in Table 1.

In all examples, atoms or beads (groups of atoms) are treated as spheres, displayed as A-Frame `<a-sphere>` components coded directly in the HTML. Residue beads for proteins are centered at CA atoms and their radii are calculated as the cubic root of their volumes as compiled in [14]. Bonds between atoms or residues are displayed as `<a-tube>` components registered by Don McCurdy's A-Frame-extras. Sphere and tube tags are affected by an id that gives handlers for subsequent operations, and are placed inside `<a-marker>` tags, which are components registered by the A-Frame-compatible AR.js to handle AR markers.

The examples provided here use the Hiro and Kanji markers built-in inside AR.js. One or more marker tags are located inside one `<a-scene>` tag, which includes also a `<a-entity camera>` tag to locate a camera for rendering. Style definitions at the beginning of the HTML file setup the video feedback and display. Video can be horizontally flipped or not through transforms depending on the relative orientation of the user, the computer webcam or smartphone camera, and the screen or projection.

Table 1. Client-side libraries, APIs and components used to build the web apps reported here.

Tool	URL
AR.js	https://github.com/jeromeetienne/AR.js
A-Frame	https://aframe.io/
Three.js	https://threejs.org/
Cannon.js through A- Frame physics	http://www.cannonjs.org/ and https://github.com/donmccurdy/aframe-physics-system
Annyang	https://github.com/TalAter/annyang
Google Charts	https://developers.google.com/chart/

3 PROOF-OF-CONCEPT WEB APPS

This section presents sample web apps (compatible with all major web browsers in modern smartphones, tablets and computers) that introduce features of increasing complexity, organized in a first set that involves small molecules and a second set that involves proteins. Table 2 lists the URLs to the specific examples mentioned, also organized together with other relevant resources and with video examples at <https://lucianoabriata.altervista.org/jsinscience/aris/armodeling/>. Users interested in developing their own HTML web apps can use the tools provided in that website under "Building tools", continuously updated as more complex examples are developed and new features added. When using these building tools, atomic coordinates must be provided in PDB format. PDB files for proteins can be downloaded from the Protein Data Bank and related resources [15] while small molecules can be built with Hack-a-Mol at <https://chemapps.stolaf.edu/jmol/jsmol/hackamol.htm>, a tool based itself on client-side web software like JSmol [16] and JSME [17].

3.1 Small molecules

3.1.1 Simplest, HTML-only examples

The simplest web app example consists exclusively of HTML code (Table 2A). With it, the user drives a lysine side chain with the Hiro marker and a glutamate side chain with the Kanji marker. Each molecule is anchored to the center of its corresponding AR marker through its CA atom. Their protonation states correspond to neutral pH, so lysine is protonated hence its N atom (blue) is charged by +1, whereas glutamate is deprotonated hence its O atoms (red) bear a total charge of -1. These charges do not have any effect on this example, but they do in the examples B and C.

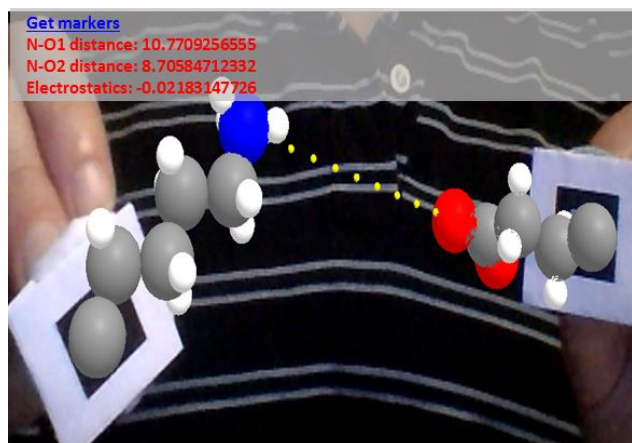


Figure 1: Example B from Table 2, two small molecules driven in space with AR markers, augmented with simple calculations in real time.

Table 2. Links to the example web apps about small molecules.

Web app	URL
A) HTML-only small molecules	https://lucianoabriata.altervista.org/jsinscience/arjs/armodeling/smallmolsimplest.html
B) (A) plus clash detection	https://lucianoabriata.altervista.org/jsinscience/arjs/armodeling/smallmolclashdetection.html
C) (B) with phone vibration	https://lucianoabriata.altervista.org/jsinscience/arjs/arjs-phones.html
D) (B) with proton transfer	https://lucianoabriata.altervista.org/jsinscience/arjs/armodeling/smallmolprotontransfer.html
E) Diels Alder reaction	https://lucianoabriata.altervista.org/jsinscience/arjs/armodeling/smallmoldielsalder.html
F) Glucose enantiomers and isomers	Linear L- vs. linear D- glucose: https://lucianoabriata.altervista.org/jsinscience/arjs/armodeling/smallmolLglcDglc.html D-furanose vs. D-pyranose: https://lucianoabriata.altervista.org/jsinscience/arjs/armodeling/smallmolglcfurapyra.html

3.1.2 Adding chemistry and physics with JavaScript

Example B (Figure 1) features the same two molecules as example A, but includes simple JavaScript code to (i) adapt the positions of 10 yellow spheres that make up a dotted line connecting in space the lysine's N atom with one of the glutamate's O atoms; (ii) report the distance between these 2 atoms and the corresponding attractive electrostatic force in real time; and (iii) test and display clashes between any pair of atoms of the two molecules. The code for (i) is wrapped inside the dashedline.js file; whereas the code for (ii) and (iii) is located between <script> tags at the end of the HTML file. The distance, electrostatic and clash calculations are inside a setInterval() function that is executed every 200 ms and uses the id identifiers of the sphere tags to locate them.

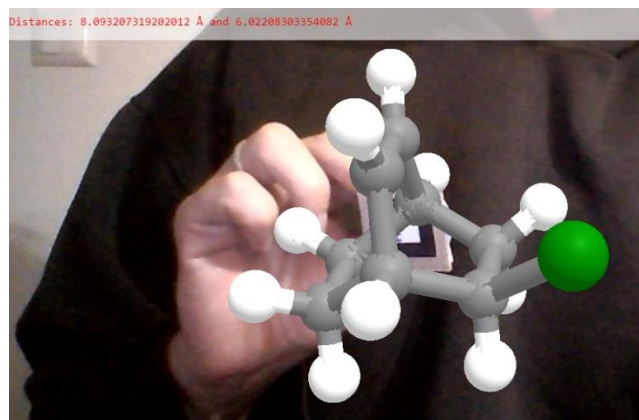


Figure 2: The bicyclic product of the reaction in example E, where carbon atoms are grey, hydrogens white and chlorine green.

The distance is calculated in Angstrom and includes a correction for a zoom factor that scales atom sizes and positions when the molecular coordinates are parsed into A-Frame HTML, to properly fit the screen (in this example a factor of 2). Clashes are detected as two spheres being within 3 Å, and displayed as semitransparent A-Frame spheres centered on the affected atoms.

Example C is the same as B but is more suited for phones, as it executes a 200 ms long vibration when a clash is detected. Also, its video display is flipped horizontally compared to the other examples, to allow use with commodity AR lenses such as Google Cardboard.

3.1.3 Simulating chemical reactivity

Example D extends example B by incorporating a very simplistic version of distance-based proton transfer. As explained in 3.1.1, the lysine side chain is protonated and the glutamate side chain is deprotonated. Example D uses JavaScript to stochastically transfer one proton from lysine's N atom to one of the O atoms of glutamate if the lysine is protonated, or the other way around. Proton transfers occur only when the proton is within 2 Å of the receiving N or O atom, and jumps back and forth to reflect 70% time-averaged population of protonated lysine and 30% of protonated glutamate, to convey the feeling of different acidic constants. At distances longer than 2 Å but shorter than 3 Å the web app displays a yellow dotted line that represents a hydrogen bond between the potential receiver heavy atom and the involved proton.

Example E would allow teachers to illustrate stereoselectivity in the Diels-Alder reaction. This

reaction occurs between a dienophile and a conjugated diene. It takes place in a concerted fashion, so the side of the diene where the initial approach occurs defines the stereochemistry of the product. The web app in this example allows users to visualize all this in 3D as they approach a molecule of 1,3-cyclohexadiene held in the left hand (Hiro marker) and a molecule of vinyl chloride in the right hand (Kanji marker). As the two pairs of reacting C atoms approach simultaneously, the two new bonds gain intensity until the product is formed. The product formed in this reaction is by itself an interesting molecule to visualize and move around in 3D through AR, because it contains two fused six-membered rings which are often hard to grasp in 2D (Figure 2).

It is very important regarding this section on reactivity, that novel machine learning methods to approximate quantum calculations through extremely fast calculations (like in [18]–[20]) could in a near future be coupled to AR systems to interactively explore reactivity with realistic energy profiles in real time, useful not only for education but also for actual research, for example to interactively test the effect of chemical substituents on a reaction, estimate effects on spectroscopic observables, probe effects of structural changes on molecular orbitals, etc.

3.1.4 Other web-based AR examples for small molecules

Visualization in 3D helps immensely to grasp the geometric details of complex small molecules and concepts about chirality, planarity and nonplanarity, rings, etc. The main website contains, under the “Small molecules” menu, other examples on top of those described here, that allow exploration of 3D structures in molecules like glucose in its multiple forms, among others.

3.2 Biological macromolecules

Biological macromolecules include large covalent polymers like proteins, nucleic acids and storage sugars, as well as non-covalent assemblies such as lipids forming membranes and complexes of different kinds of macromolecules, like ribonucleoproteins or integral membrane proteins.

Macromolecules can be modeled *in silico* either explicitly accounting for all their atoms (atomistic models) or by grouping atoms into beads, in the so-called coarse-grained models. Such grouping

into beads decreases the number of particles to be simulated dramatically, and reduces the degrees of freedom of the system, thus overall reducing the mathematical complexity of the system. Common coarse-graining schemes include grouping four heavy atoms and their attached hydrogens into a single bead, or even representing each unit of the polymer as a single sphere. So far the tools available at the website allow treating proteins either at atomistic resolution, by using the same building tool developed for small molecules, or at two coarse-grained levels, either 1 bead per residue (centered at CA atoms), or 2-to-4 beads per residue separating backbone from side chain to deliver more realistic shape than 1 bead per residue (similar to the MARTINI[21] coarse-graining scheme).

3.2.1 HTML-only AR for proteins at atomistic and coarse-grained descriptions

For small proteins, or sections of large proteins, atomistic representations are useful and can be well displayed even in smartphones. Examples A and B from Table 3 use HTML only and were built from PDB structures using the same small molecule builder web app used in section 3.1 for small molecules, with the only remark that molecules were first centered at 0,0,0 in an external program, here VMD[22].

Table 3. Links to example web apps dealing with protein systems.

Web app	URL
A) Protein secondary structures	https://lucianoabriata.altervista.org/jsinscience/arjs/armodeling/secondarystructures.html
B) Standing alpha helix	https://lucianoabriata.altervista.org/jsinscience/arjs/armodeling/bigalphahelix.html
C) Two proteins in atomic detail	https://lucianoabriata.altervista.org/jsinscience/arjs/armodeling/ubiquitinandNESatomistic.html
D) Ubiquitin-UIM, 1 bead/res.	https://lucianoabriata.altervista.org/jsinscience/arjs/armodeling/ubiquitinuimsimplest.html
E) (D) with active restraints and contact force field	https://lucianoabriata.altervista.org/jsinscience/arjs/armodeling/ubiquitinuimforcefieldandvoic.html
F) (E) with real-time comparison of SAXS profile	https://lucianoabriata.altervista.org/jsinscience/arjs/armodeling/ubiquitinuimffvoicesaxs.html
G) (D) with proteins connected through flexible linker	https://lucianoabriata.altervista.org/jsinscience/arjs/armodeling/ubiquitin-uim-cannon.html

Example A from Table 3 displays on the Hiro marker a canonical alpha helix made up of consecutive alanine residues interrupted with a

proline (Figure 3), and on the Kanji marker a beta-hairpin from an actual NMR structure (PDB ID 2k6v[23]), both in atomic detail including the hydrogen atoms (excluding side chains to better show the backbone hydrogen bonds). These examples allow 3D exploration of the two main kinds of secondary structures found in proteins, readily highlighting the strong $i-i+4$ hydrogen bonds in alpha helices, the trans-beta-sheet hydrogen bonds of antiparallel beta strands, the role of prolines as alpha helix breakers, and the twisted nature of beta hairpins.

In particular, example B (Figure 3) presents a standing helix that can be visualized from a Hiro marker lying on a flat surface, such that teachers and surrounding students can concurrently inspect it as exemplified in the figure.

Example C from Table 3 displays on the Hiro marker an NMR structure of ubiquitin (PDB ID 1d3z[24], model 1), and on the Kanji marker a helical model of the nuclear export signal of *Arabidopsis thaliana* Argonaute 1 protein [25] (Figure 4). Both visualizations include also a CA trace colored black, computed with another web app of the “Building tools” menu. For simplicity, the hydrogen atoms are omitted in these examples. The ubiquitin example allows exploration of a small but complete protein structure, that could be further augmented to show residue names and details like non-covalent interactions, leading to a complete interactive 3D resource on protein structure. On the other hand, the example about the helical nuclear export signal readily shows the functionally relevant amphipathic nature of these protein motifs.

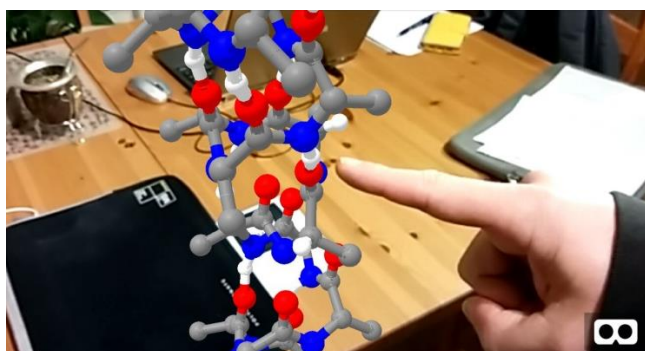


Figure 3: Example B from Table 3, a standing alpha helix as seen through an Android smartphone in mobile Chrome. H atoms are in white, O in red, N in blue and C in grey. The icon in the bottom right splits the screen in two for stereo projection in commodity AR lenses.

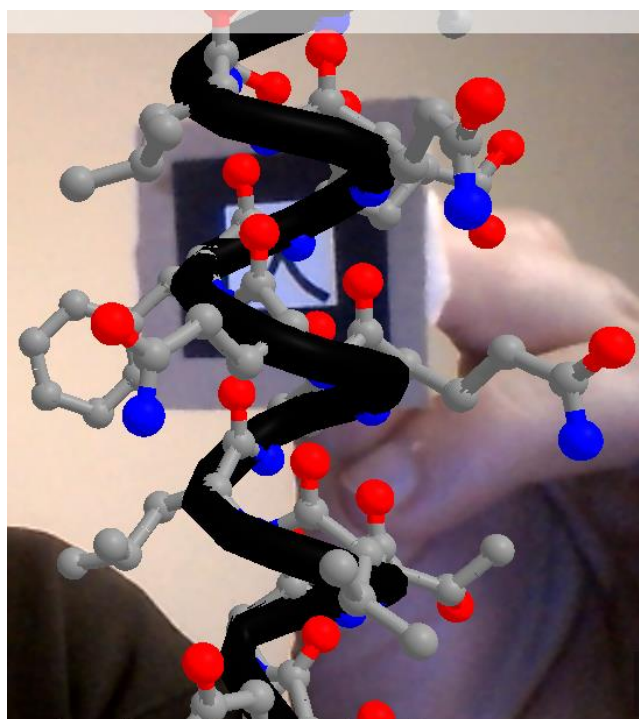


Figure 4: The nuclear export signal from example B in Table 3, modeled as an alpha helix, shows three hydrophobic residues on the left face and polar residues on the right.

Example D deals again with ubiquitin, this time represented at a coarse-grained level of 1 bead per residue, and a ubiquitin-interacting motif of helical structure, also represented at 1 bead per residue. The beads are colored according to amino acid type (blue = positively charged, red = negatively charged, green = polar uncharged, and grey = hydrophobic). They are semitransparent except for one bead from each protein that is opaque; these two define a restraint coordinate for non-covalent interaction depicted as a yellow dashed line that connects them in space.

3.2.2 Restraints, force fields and match to experimental data for interactive, integrative modeling of proteins

Example D just introduced is the starting point for more complex cases where ubiquitin and its interacting partner are subject to molecular modeling calculations coded in JavaScript. Such kinds of calculations form the core of computer-based studies of structure and function in biological macromolecules.

The first of these examples, E in Table 3, incorporates a rudimentary residue-level force field for clash detection and a whole-molecule-based force to apply restraints. Clashes between

beads of the two proteins are manifested as more opaque colors. The restraint is applied on the interacting partner, along the coordinate shown as a yellow dotted line. These calculations involve iteration through all possible pairs of beads representing each protein's residues, computing distances and updating display (molecule positions and bead opacity) accordingly.

Example F (Figure 5) goes one step further into actual uses that these technologies could have in structural biology and molecular modeling. Building from example E, it incorporates on-the-fly calculation of small angle X-ray scattering (SAXS) profiles for the protein mixture and compares this profile to an experimental reference, offering a way to test possible docking poses that are compatible with the experimental data. The SAXS profile calculation is based on the Debye formula iterated through pairs of residues instead of iterating through all atoms as the full equation requires, for simplicity and speed. It should be noticed though that realistic SAXS profiles of high utility can be achieved by using just two scattering bodies per residue[26], a finding that enables realistic, detailed, real-time SAXS calculations of true utility in the near future.

In examples E and F, since the user's hands are both busy handling the AR markers, control of the clash-detection force field, restraint application, and SAXS calculations is achieved through spoken commands in English language, processed through the browser's speech recognition API. The possibility of incorporating such feature illustrates the superb integration capacity of libraries for client-side scripting for the browser.[11]

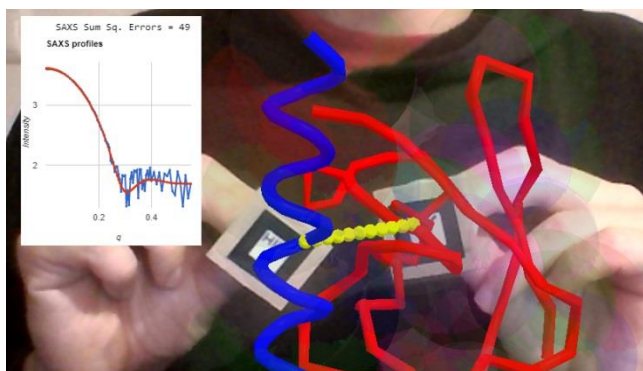


Figure 5: Ubiquitin (red trace) and ubiquitin-interacting motif (blue) driven in 3D with two AR markers, as the web app computes the predicted SAXS profile and displays it overlaid on top of an experimental (simulated with noise) profile, together with a metric of the fit quality.

3.2.3 Realistic handling of flexible interdomain linkers in proteins

Molecular motions, “dynamics” are essential for protein function and regulation, and certainly a feature that advanced modeling platforms must offer. Broadly speaking, such dynamics range from restricted, coordinated structural changes in ordered domains, to extended dynamics in very flexible regions. Correctly accounting for dynamics across that vast range of time and size scales is an active goal of research in molecular dynamics simulation methods, and requires complex force fields and molecular dynamics engines. Very encouragingly, a recent article showed that it is feasible to code such simulation methods in JavaScript [27] achieving near-native performance. For AR applications, though, a number of yet unclear modifications are required in standard molecular dynamics engines that make them compatible with user-driven moves of the molecules; thus this is an area that requires research and probably a series of alternative solutions tailored to different problems.

The examples proposed here consider only the dynamics of very flexible linkers within the very coarse approximation that beads describing amino acids are rigid spheres connected by fixed distances. In the examples, this is handled very efficiently through the Cannon.js software, wrapped through the A-Frame-physics extension. Example G is based in ubiquitin and its interacting partner as in D but in a fictitious scenario where they are covalently connected by 6 amino acids that form a flexible linker connecting ubiquitin's C-terminus to the partner's N-terminus (Figure 6). Here, each globular domain (corresponding to ubiquitin or the interacting helix) is modelled with 2- to 4- beads per residue, while the flexible linker is modelled as backbone beads only. Such very simple model can help to answer complex questions related to the separation of the anchor points and the maximal extension of the linker when straight, for example: How far can the two proteins go with the given linker? Can the interacting partner be docked to satisfy the restraint yet allowing for a relaxed configuration of the linker? More complex settings could in turn apply repulsion between the globular domains, compute experimental observables to match in real time like in the SAXS example shown before, etc.

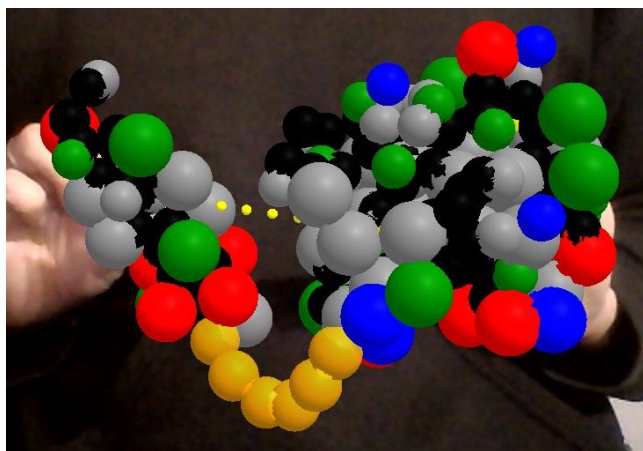


Figure 6: From example G, ubiquitin and ubiquitin-interacting motif modelled as 2-4 beads per residue, colored by physiochemical properties (grey=hydrophobic, red=negative, blue=positive, green=polar uncharged) driven in 3D with two AR markers and with their termini connected through a flexible linker of six backbone-sized beads (orange).

4 DISCUSSION AND CONCLUSION

The examples introduced here advance a true potential for AR and VR technologies in education and research. In education, such tools can replace/complement tangible modeling kits by allowing virtually unlimited numbers and kinds of atoms, augmenting models with additional information such as forces, charges, electron clouds and orbitals, data facts, etc. In research, such tools can help to visualize and probe molecular structure, simulate expected outcomes of experiments and test them against experimental data, etc., everything through intuitive cues and interactions. The web portal at <https://lucianoabriata.altervista.org/jsinscience/aris/armodeling/> includes even more examples about using AR for education and research involving small and macromolecules, such as interactive protein-protein docking from coevolution data (with a specific example from [28]) and interactive exploration of paramagnetically-induced chemical shifts in nuclear magnetic resonance).

The near future will likely see these tools blended with modern molecular simulations and visualization methods, resulting in fully-fledged programs for deeply interactive, immersive molecular modeling experiences that overcome the severe limitations of traditional software based on screens, mouse and keyboards. Furthermore, happening all through the web will seamlessly enable online collaboration [29] among multiple

peers as well as between students and teachers. Adding 3D lenses, haptic devices for force feedback, speech-based voice commands, numerical simulations and intelligent data and text mining will then bring research and education to the next level where human thought and intent couple with computer power to get the best out of both worlds.

ACKNOWLEDGEMENTS

I acknowledge all the developers of the client-side web tools listed in Table 1, as well as the very helpful communities who contribute to their improvement, bug detection and correction, documentation, and online help.

I also acknowledge numerous researchers from the chemistry, physics and biology communities who have contributed several useful ideas and suggestions, most of them inspiring some of the presented, as well as future, examples.

REFERENCES

- [1] A. Gillet, M. Sanner, D. Stoffler, D. Goodsell, and A. Olson, "Augmented reality with tangible auto-fabricated models for molecular biology applications," *IEEE Visualization*, 2004.
- [2] A. Gillet, M. Sanner, D. Stoffler, and A. Olson, "Tangible interfaces for structural molecular biology," *Struct. Lond. Engl.* 1993, vol. 13, no. 3, pp. 483–491, Mar. 2005.
- [3] S. I. O'Donoghue *et al.*, "Visualizing biological data—now and in the future," *Nat. Methods*, vol. 7, no. 3 Suppl, pp. S2–4, Mar. 2010.
- [4] M. Krichenbauer, G. Yamamoto, T. Taketom, C. Sandor, and H. Kato, "Augmented Reality versus Virtual Reality for 3D Object Manipulation," *IEEE Trans. Vis. Comput. Graph.*, vol. 24, no. 2, pp. 1038–1048, Feb. 2018.
- [5] C. Berry and J. Board, "A Protein in the palm of your hand through augmented reality," *Biochem. Mol. Biol. Educ. Bimon. Publ. Int. Union Biochem. Mol. Biol.*, vol. 42, no. 5, pp. 446–449, Oct. 2014.
- [6] J. C. Vega Garzón, M. L. Magrini, and E. Galembeck, "Using augmented reality to teach and learn biochemistry," *Biochem. Mol. Biol. Educ. Bimon. Publ. Int. Union Biochem. Mol. Biol.*, Apr. 2017.
- [7] P. Wolle, M. P. Müller, and D. Rauh, "Augmented Reality in Scientific Publications—Taking the Visualization of 3D Structures to the Next Level," *ACS Chem. Biol.*, vol. 13, no. 3, pp. 496–499, Mar. 2018.
- [8] M. Fjeld and B. M. Voegtli, "Augmented Chemistry: an interactive educational workbench," in *Proceedings. International Symposium on Mixed and Augmented Reality*, 2002, pp. 259–321.
- [9] H. E. Pence, A. J. Williams, and R. E. Belford, "New Tools and Challenges for Chemical Education: Mobile Learning, Augmented Reality, and Distributed Cognition in the Dawn of the Social and Semantic Web," in *Chemistry Education*, Wiley-VCH Verlag GmbH & Co. KGaA, 2015, pp. 693–734.
- [10] L. A. Abriata, J. P. G. L. M. Rodrigues, M. Salathé, and L. Patiny, "Augmenting research, education and outreach with client-side web programming," *Trends Biotechnol.*, 2017.
- [11] L. A. Abriata, "Web Apps Come of Age for Molecular Sciences," *Informatics*, vol. 4, no. 3, p. 28, 2017.
- [12] P. Maier, M. Tönnis, and D. GudrunKlinker, "Dynamics in Tangible Chemical Reactions," 2009.

- [13] P. Maier and G. Klinker, "Augmented Chemical Reactions: 3D Interaction Methods for Chemistry," *Int. J. Online Eng.*, vol. 9, 2013.
- [14] L. A. Abriata, T. Palzkill, and M. Dal Peraro, "How structural and physicochemical determinants shape sequence constraints in a functional enzyme," *PLoS One*, vol. 10, no. 2, p. e0118684, 2015.
- [15] L. A. Abriata, "Structural database resources for biological macromolecules," *Brief. Bioinform.*, Jun. 2016.
- [16] R. M. Hanson, J. Prilusky, Z. Renjian, T. Nakane, and J. L. Sussman, "JSmol and the Next-Generation Web-Based Representation of 3D Molecular Structure as Applied to Proteopedia," *Isr. J. Chem.*, vol. 53, no. 3–4, pp. 207–216, 2013.
- [17] B. Bienfait and P. Ertl, "JSME: a free molecule editor in JavaScript," *J. Cheminformatics*, vol. 5, p. 24, 2013.
- [18] J. S. Smith, O. Isayev, and A. E. Roitberg, "ANI-1: an extensible neural network potential with DFT accuracy at force field computational cost," *Chem. Sci.*, vol. 8, no. 4, pp. 3192–3203, Apr. 2017.
- [19] F. M. Paruzzo, A. Hofstetter, F. Musil, S. De, M. Ceriotti, and L. Emsley, "Chemical Shifts in Molecular Solids by Machine Learning," *ArXiv*, vol. 1805, p. 11541.
- [20] A. P. Bartók *et al.*, "Machine learning unifies the modeling of materials and molecules," *Sci. Adv.*, vol. 3, no. 12, Dec. 2017.
- [21] S. J. Marrink, H. J. Risselada, S. Yefimov, D. P. Tieleman, and A. H. de Vries, "The MARTINI force field: coarse grained model for biomolecular simulations," *J. Phys. Chem. B*, vol. 111, no. 27, pp. 7812–7824, Jul. 2007.
- [22] W. Humphrey, A. Dalke, and K. Schulten, "VMD – Visual Molecular Dynamics," *J. Mol. Graph.*, vol. 14, pp. 33–38, 1996.
- [23] L. A. Abriata *et al.*, "Mechanism of Cu(A) assembly," *Nat. Chem. Biol.*, vol. 4, no. 10, pp. 599–601, Oct. 2008.
- [24] G. Cornilescu, J. L. Marquardt, M. Ottiger, and A. Bax, "Validation of Protein Structure from Anisotropic Carbonyl Chemical Shifts in a Dilute Liquid Crystalline Phase," *J Am Chem Soc*, vol. 120, pp. 6836–6837, 1998.
- [25] N. G. Bologna *et al.*, "Nucleo-cytosolic Shuttling of ARGONAUTE1 Prompts a Revised Model of the Plant MicroRNA Pathway," *Mol. Cell*, vol. 69, no. 4, p. 709–719.e5, Feb. 2018.
- [26] K. Stovgaard, C. Andreatta, J. Ferkinghoff-Borg, and T. Hamelryck, "Calculation of accurate small angle X-ray scattering curves from coarse-grained protein models," *BMC Bioinformatics*, vol. 11, p. 429, Aug. 2010.
- [27] C. Jiang and X. Jin, "Quick Way to Port Existing C/C++ Cheminformatics Toolkits to the Web Using Emscripten," *J. Chem. Inf. Model.*, Sep. 2017.
- [28] S. Ovchinnikov, H. Kamisetty, and D. Baker, "Robust and accurate prediction of residue-residue interactions across protein interfaces using evolutionary information," *eLife*, vol. 3, p. e02030, 2014.
- [29] L. A. Abriata, "Concurrent interactive visualization and handling of molecular structures over the Internet in web browsers," *ArXiv E-Prints*, Dec. 2017.